JOURNAL OF MATERIALS SCIENCE 32 (1997) 2655–2660

Characterization of aluminium coated poly(ethylene terephtalate) films by acoustic microscopy

B. CROS*
LTM, IPSé, 90010 Belfort Cedex, France

M. F. VALLAT
ICSI, BP2488, 68057 Mulhouse Cedex, France

F. AUGEREAU
LAIN, Université Montpellier II, 34095 Montpellier Cedex 05, France

Poly(ethylene terephtalate) (PET) films coated with thermally evaporated aluminium are studied by acoustic microscopy after various thermal treatments. Three types of contrasts are observed on acoustic images which are interpreted in terms of the acoustic signature results. The first type of contrast behaviour is explained by the presence of ceramic particles. The second type of contrast behaviour can be characterized by the modelling of the Al/PET system as being adhesion defects. The formation of cyclic oligomers at the PET film surface during the thermal processing is envoked to explain the third type of contrast behaviour. Changes in films produced by thermal processing can thus be followed by acoustic imaging.

1. Introduction

Microacoustic techniques, such as microechography and acoustic microscopy, have been shown to be excellent techniques for the study of polymer crosslinking [1]. The velocity of the acoustic waves is closely related to the elastic properties of the investigated solid (and also to its density) [2]. The crosslinking, sharply increases the Young's modulus by increasing the number of strong bonds between the polymer chains, [3]. Microechography has been used to map the elastic properties of polymers. It permits the control of mask transfer by highlighting the occurance of any resolution loss, attenuation or skin effect [4]. However, microechography does not provide the same level of performance as that of acoustic microscopy since the transducer is not strongly focused and the lateral resolution is lower. In addition the propagation velocity of Rayleigh waves or longitudinal waves can not be measured locally.

Thin films of poly(ethylene terephtalate) (PET) have many applications due to their excellent mechanical properties. For packaging applications, they are coated with aluminium which acts as an oxygen barrier. The aim of this work is to characterize the PET films, their thermal behaviour and their adhesion with the metallic coating. The typical structure of polymers and the existence of secondary bonds produces the strong absorption of acoustic waves observed for polymers. Their study requires a trade off to be made between the use of high frequencies, which increases the resolution of the technique, and low frequencies which lessens the attenuation by the material.

2. Experimental procedure

2.1. The acoustic microscopy technique

The acoustic microscopy technique is a well known non-destructive method [5] to characterize a range of materials as diverse as metallic alloys and ceramics with amorphous [6] or porous [7] microstructures. The acoustic microscope uses an acoustic beam focused by a spherical lens. It can operate in imaging mode or be used to perform local measurements. The images are recorded by scanning the sample in a xy plane perpendicular to the transducer and to the acoustic beam. In microanalysis of the elastic structure of surfaces and subsurfaces, the microscope is used to measure the elastic properties via the acoustic signature $V(z)$ of the material. The acoustic signature is achieved by moving the sample along the axis from the focal plane towards the acoustic lens and recording the reflected acoustic signal variation as a function of the sample defocusing z [5]. The output voltage $V(z)$ returned by the transducer displays pseudooscillations, which represent the materials acoustic signature. Leaky waves such as surface acoustic waves, surface skimming longitudinal waves (SSLWs) and Lamb waves can be associated with interference phenomena in the $V(z)$ curves. Often, a single mode appears that can dominate any other mode. The $V(z)$ response can be quantified through the fast Fourier transform method which currently finds application in numerical signal processing. It gives the period of the pseudo-oscillations and thus the velocities (V) of the various acoustic modes can be calculated from the

* Present address: LAIN, CC082, Université Montpellier II, 34095 Montpellier Cedex 05, France Email: cros@lain.Univ-montp2.fr

formula [5, 8]:

$$V = V_0[1 - (1 - V_0/2f\Delta z)^2]^{-1/2} \quad (1)$$

where V_0 is the velocity in the coupling fluid, f is the operating frequency and Δz is the period of the pseudo-oscillations. Since the surface waves are highly sensitive to the properties of the sample, the $V(z)$ response can give valuable information about local changes in the material.

The high frequency (600 MHz) acoustic microscopy technique has been chosen as the investigative probe in this work due to its resolution, about 2–3 μm in focus, and also the characteristics of the material of interest namely that the velocity of acoustic waves in PET is amongst the highest in polymers ($V_L = 2540\ m\ s^{-1}$) and are in the detection domain of the apparatus. Since the area we wish to characterize is a superficial layer of few microns thickness then we will not encounter any problems with damping of the acoustic waves.

2.2. The materials

The 12 μm thick PET films (Mylar® from DuPont) were coated with a 40 nm thick aluminium layer using the thermal evaporation technique. Adhesion measurements of such assemblies are difficult due to the thickness and properties of the metal layer. The application of a technique based on ultrasonic vibration which ejects metal particles in to a liquid medium has shown that it is possible to quantify the adhesive behaviour [9]. Also under constant evaporation conditions, a thermal treatment of strained metallized samples leads to an improved adhesive behaviour [10]. This improvement depends on the time and the temperature of the heat treatment; the higher the temperature the larger the improvement. However, the variation is limited by the heat setting conditions applied during the processing of the PET film. Typically, the optimum behaviour is observed for treatments at around 200–230 °C for 10–20 min. These thermal treatments do not only modify the interfacial polymer/aluminium properties but also the bulk properties of both the PET and aluminium. It is however quite difficult to isolate the respective contributions of the contributing factors.

3. Results

3.1. The acoustic images

The acoustic images for all samples display local contrasts with an almost circular geometry with a diameter of 2–4 μm (Fig. 1). We designate them as type A behaviour. At high magnification, they appear to have 3 aspects, with darker or brighter shades (corresponding to low or high amplitude respectively) than the background and sometimes surrounded by a halo (Fig. 2).

Other dark shaded contrasts are observed whose dimensions can exceed 30 μm. They are of two kinds that are designated as type B and C behaviour. The *B* contrasts appear before the thermal processing in the PET films coated with aluminium. They exhibit quite regular shapes and sharp edges (Fig. 3). They do not exist on the non-coated sides and their number decreases when the samples are heated for longer times and at higher temperatures. The type C contrasts are observed in films heated at temperatures greater than 200 °C for more than 15 min. Their shape

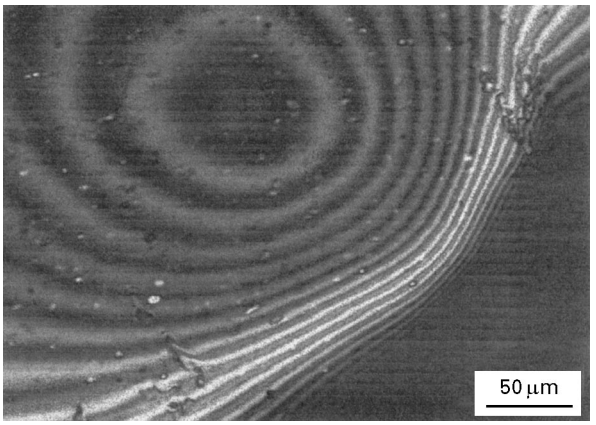

Figure 1 Acoustic image ($500 \times 350\ \mu m^2$) of the surface of the PET film coated by a 0.04 μm aluminium layer. The contrasts (of type *A*) are interpreted as ceramic particles. Their aspect depends on their position in relation to the focal plane. The fringes reveal slight defects in planarity.

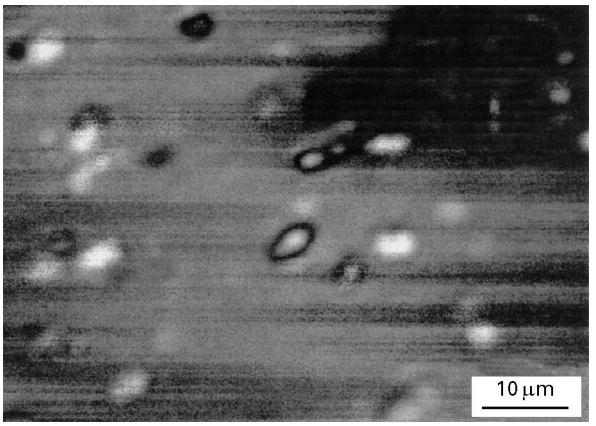

Figure 2 High magnification acoustic image ($100 \times 70\ \mu m^2$) achieved by focusing 9 μm below the surface of the film.

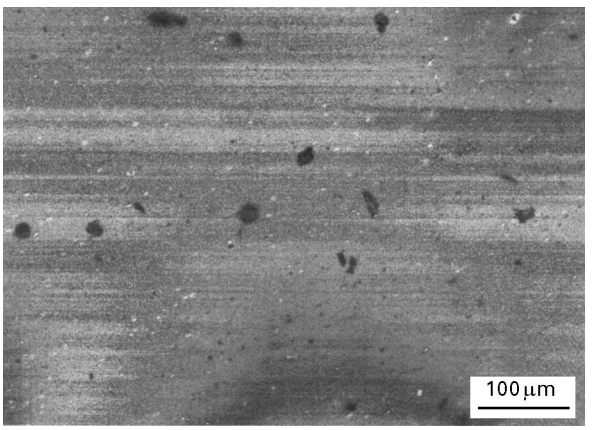

Figure 3 Acoustic image ($1000 \times 700\ \mu m^2$) of the surface of the PET/aluminium assembly before thermal treatment. The dark contrasts of type *B* are interpreted as unbonded areas.

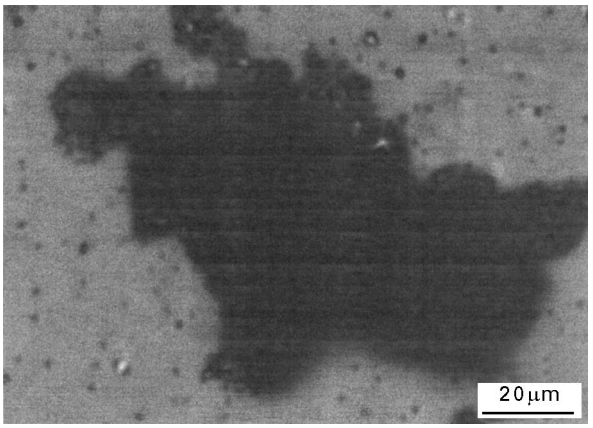

Figure 4 Acoustic image ($200 \times 140\ \mu m^2$) of the PET surface after a 20 min heat treatment at 230 °C displaying a dark *C* type contrast.

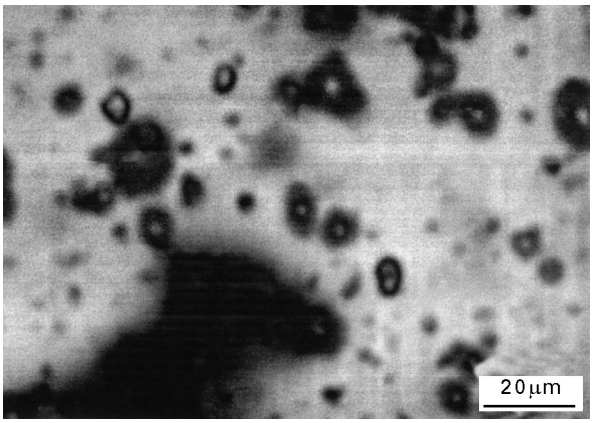

Figure 5 Acoustic image ($200 \times 140\ \mu m^2$) of *C* type contrast surrounding ceramic particles (PET heated at 230 °C for 20 min).

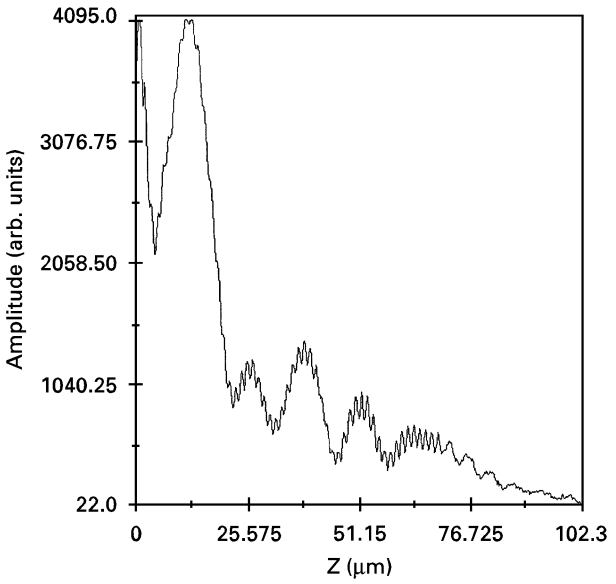

Figure 6 Acoustic signature performed on a bright A type contrast of an aluminium coated PET sample before thermal treatment.

is typically indented and they do not have sharp outlines (Fig. 4). Moreover, they do not mask the A type contrasts, but instead they surround them (Fig. 5).

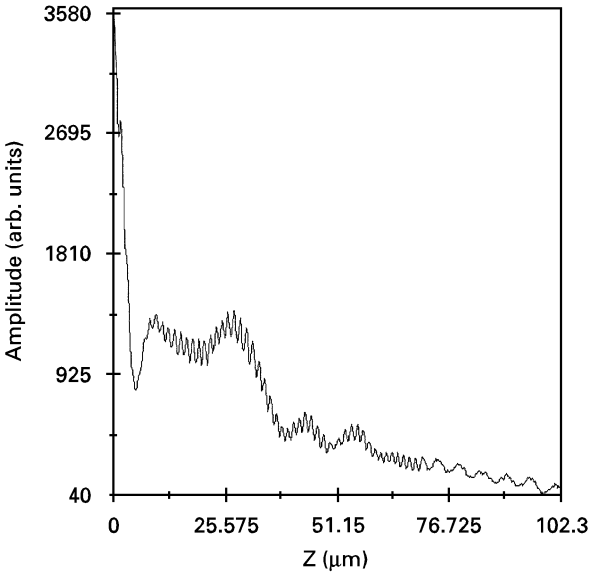

Figure 7 Acoustic signature performed before thermal treatment on the background of the image of an aluminium coated PET sample.

The presence of the Al coating does not to any extent modify the image and the partially coated regions can not be distinguished.

3.2. The acoustic signature $V(z)$

The acoustic signature measurements performed on the bright regions of type *A* contrasts display arches with larger amplitudes (Fig. 6) than those measured in the background of the image (Fig. 7). The acoustic signatures measured on dark type *B* contrasts appear very damped and consist of only one or two arches. Over the C type contrasts, the echo disappears and the $V(z)$ measurement can not be performed.

4. Modelling

4.1. Modelling the Al/PET system

The acoustic wavelength in the sample (about 3 μm at 600 MHz) is much larger than the thickness of the aluminium coating (0.04 μm), thus the acoustic characteristics of the Al/PET system only relate to the characteristics of the polymer film and its interface with the metal. The experimental system has been simulated using two different models. The first model considers that the layer is thick as compared to the depth of penetration into the PET of the acoustic waves (a few microns at high frequency, typically 600 MHz, and about 100 μm at low frequency, typically 25 MHz). Consequently, the system representing the samples may be simulated by a semi-infinite model. The second model takes into account the guided waves generated by the small 12 μm thickness of the polymer film. The acoustic signature was calculated using the following input data for each layer: the longitudinal velocity V_L, the shear velocity V_T, the density and thickness. The velocities of the different modes in each model were deduced after a fast Fourier transform (FFT) treatment of the calculated $V(z)$ and they were compared to the experimentally measured

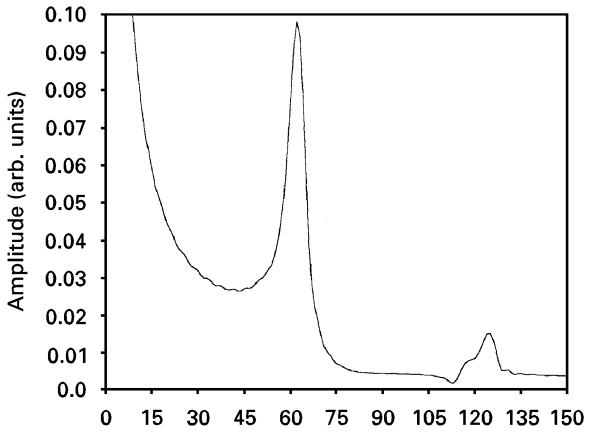

Figure 8 FFT treated spectrum of the acoustic signature calculated for a PET film modelled with a semi-infinite thickness.

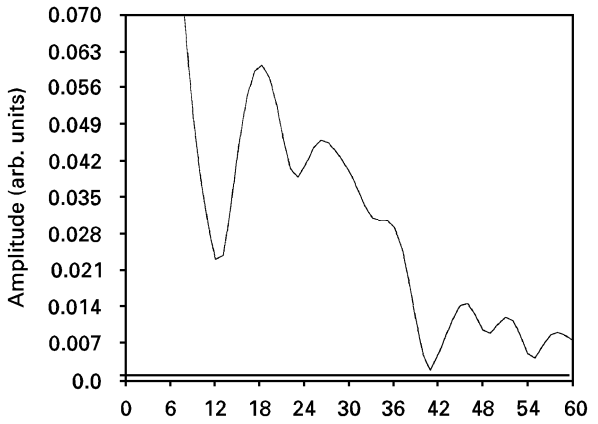

Figure 9 FFT treated spectrum of the acoustic signature calculated by modelling the system Al 0.04 μm/PET 12 μm.

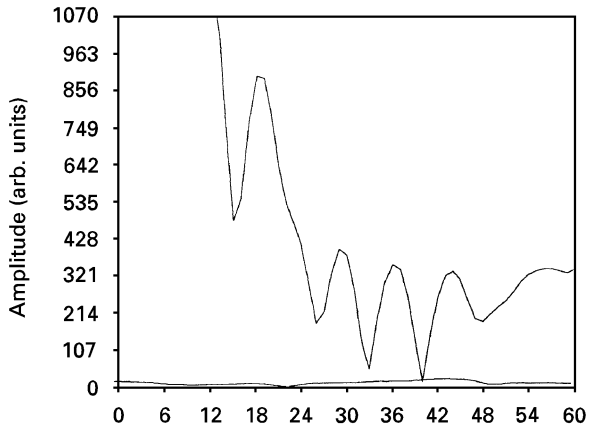

Figure 10 FFT treated spectrum of the acoustic signature performed on the background of an image of a 12 μm PET film with a 0.04 μm aluminum coating.

velocities. The model that considered the thickness of the PET film as being semi-infinite (Fig. 8) does not produce results that mimic the complexity of the experimental FFT curves. The calculation in which the correct PET thickness was used (Fig. 9), is in better agreement with the experimental results (Fig. 10). In fact, the model shows that the conditions to generate Lamb waves in a 12 μm thick layer are satisfied. Under these circumstances the wavelength of the surface mode, taking into account the increase in velocity due to the presence of ceramic particles with a high elastic constant, is about 2.5 μm. The calculations confirm that the thickness of the metallic deposit is too small to significantly modify the velocity values and therefore the images and the acoustic signature. To asses the consequences of a possible oxidation of the aluminium layer, we have simulated a complete reaction by the system Al_2O_3 0.04 μm/PET. The results show that the presence of the oxide would increase the value of V_T.

4.2. Modelling of the adhesion defects

The adhesion defects have been modelled in the same manner by using a theoretical system consisting of Al/fluid (air or water)/PET. Different kinds of adhesion conditions varying from imperfect contact to unbonding were simulated by varying the thickness of an air or water layer in successive calculations of the acoustic signature. The use of fluids such as water or air to simulate the role of the interface in the propagation of the acoustic waves across an adhesion defect is justified by the large attenuation of the transverse mode of the acoustic waves in fluids. Moreover, the longitudinal mode does not propagate in air and the unbonding case simulated by a thin air layer will largely attenuate this mode. Modelling the interface by a water layer does not involve a noticeable change of the acoustic signature, while the simulation of an adhesion defect by an air layer sharply decreases the amplitude of the arches. The velocity values deduced from the FFT treated spectra do not noticeably change as the model evolves. Nevertheless, the amplitude of the peaks significantly changes as a function of the thickness of the fictitious air layer. This parameter appears to be the most reliable indicator of unbonding characteristics.

5. Discussion

5.1. Acoustic images

The circular type A contrasts with a diameter of 2–4 μm can be explained by the presence of ceramic particles that are commonly mixed with the PET to lessen the adhesion of the polymer film with its environment. The high acoustic reflectivity observed on the images is consistent with the properties of the ceramics. The different aspects of the type A contrasts depend on the location of the particles in relation to the focal plane. If they are located in focus, they appear in clear contrast. If they are located above the focus and are therefore reached by the beam before the focal plane, they generate fringes and a halo of diameter 5–10 μm. If they are located just below the focus they appear as dark shaded areas. When the acoustic beam is focused at the film surface, they often generate fringes. A defocus condition achieved by moving the transducer away from the film surface allows us to estimate the relief which can reach values of about 1 μm. The size of the ceramic particles, smaller than 5 μm, should be measured in focus, namely

when neither halo, nor interference fringes are generated. Their density (1000 to 6000 grains per mm^2 according to the PET samples) and their distribution can be deduced from the surface and volume images.

The evolution of the density of type B contrasts with the thermal processing, has been previously published as part of a study of the evolution of adhesion [10], and we were able to identify them as unbonded areas. This assumption is validated by the disappearance of these contrasts after the dissolution of the aluminium coating by mercury. The aluminium layer is too thin to appreciably change the acoustic properties of the polymer film. However, the modification of its interface with the polymer can modify the path of the acoustic waves. An unbonded area involves the reflection of the acoustic beam and consequently, the material situated underneath the interface, namely the PET film containing the ceramic particles, do not appear on the images. Indeed, the particles are not observed inside these contrasts. The beam focused on the surface of the PET disappears. Its reappearance is sometimes obtained by focusing several microns above the surface and can be explained by an aluminium bump tearing off a thickness of PET sufficient to generate an echo. At high magnitude, interferences appear inside the type B areas (Fig. 11a and b) in agreement with this assumption.

The dark zones with indented geometry (type C contrasts) are observed on samples heated at 230 °C for 20 min conditions that give rise to the crystallization of the PET. The reflectivity of these areas is very weak and the $V(z)$ measurement can not be carried out. The dimensions of these zones can exceed 100 μm. When the beam is focused at the surface level, neither Rayleigh waves, nor skimming waves exist. The film is thick enough that in focus the reflectivity is mainly a function of the density ρ and the velocity V. High contrasts can be interpreted in terms of a large change in the product ρV. If the density of the polymer material remains constant then the contrast indicates a large variation in the velocity and, consequently, in the elastic properties. The crystallized areas, extensive, dense and with a high elastic constant, form a continuous background of large acoustic impedance. This background is not highly shaded, which demonstrates the homogeneity of the crystallized regions. The passage from the type C areas to crystallized regions takes place via a steady gradient. Samples treated at low temperatures or for a short time i.e., (230 °C for 15 min or 185 °C for 20 min) reveal low contrast images. The important modifications observed by imaging appear only in samples processed at temperatures higher than 200 °C for durations of more than 10 min (typically 20 min at 230 °C). Similarly, the aluminium coated face reveals no modifications before thermal processing. Despite the strength of the thermal treatment undergone by the PET film during the condensation of the evaporated aluminium, the affected polymer thickness is probably too small (< 1 μm) to be distinguished within the resolution of the technique. Planar defects observed by other techniques [11] have xy dimensions < 0.5 μm and are not detected by the acoustic images measured at 600 MHz (the images only show contrasts with dimensions > 2 μm). The elastic characteristics corresponding to type C areas are clearly weaker than those of the matrix of the film. Our hypothesis to explain these inhomogeneities in the elastic properties is the formation of cyclic oligomers at the surface of the samples, a phenomenon well known in PET. Their thickness is small and as such they do not mask the ceramic grains but instead surround them (Fig. 4). These cyclic oligomers have poor mechanical characteristics and a weak cohesion with the matrix. They are linked to the PET only by very weak secondary bonds that are not able to ensure the coherence of the mechanical properties and the acoustic wave propagation. The appearance of C type contrasts has been reproduced on the surface of a 350 μm thick PET film, processed for 20 min at 230 °C (Fig. 12), but not at lower temperatures or shorter times.

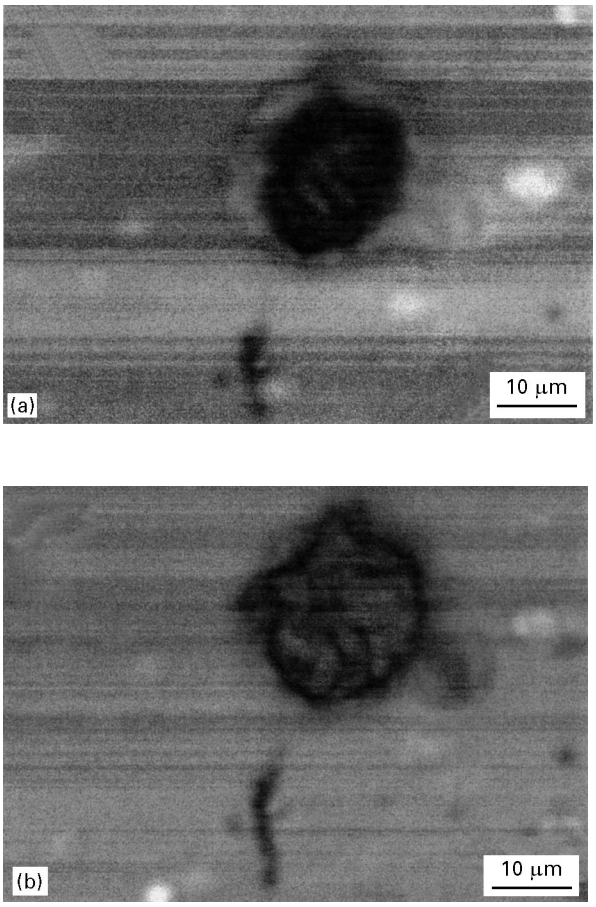

Figure 11 High magnification acoustic images (100×70 μm^2) of a contrast interpreted as an unbonded area (a) focused on the sample surface and (b) focused 1.1 μm above the sample surface.

Our interpretation of the type B and C is consistent with their absence on the non-coated side of the PET films observed before the thermal processing (Fig. 13).

5.2. Acoustic signatures

The velocity values deduced from the acoustic signatures only vary to a small extent whatever the region chosen to carry out the measurements. This consistency in values can be explained by taking into account the volume of the sample used to measure the acoustic

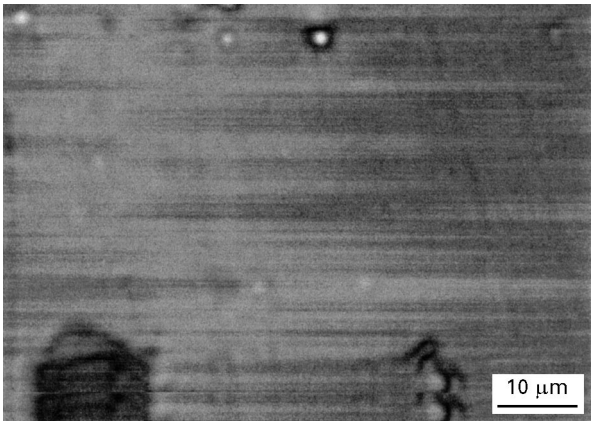

Figure 12 Acoustic image ($100 \times 70\ \mu m^2$) of the surface of a 350 μm thick PET film processed at 230 °C for 20 min.

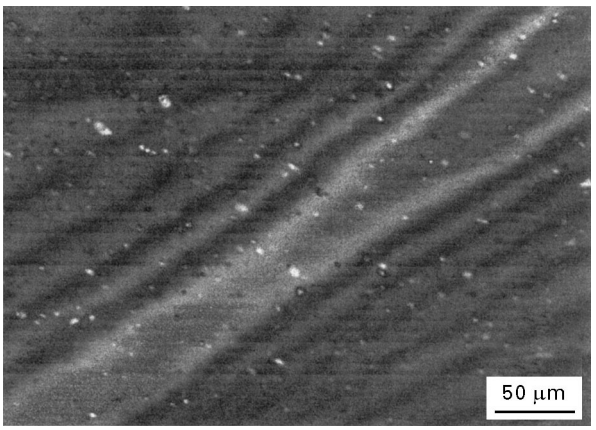

Figure 13 A slightly defocused (5 μm) acoustic image ($500 \times 350 \mu m^2$) of the non-coated side of a 12 μm PET film observed before thermal processing.

signature. On the other hand, the value of the spectral amplitude of the considered peak is highly sensitive to the chosen position. The decrease in the amplitude observed for both experimental and modelled unbonded areas is the typical characteristic of these regions.

Differences between the experimental and modelling results are apparent. The model considers that the multilayer system is homogeneous in xy over all the surface scanned by the beam during the acquisition of the acoustic signature. The models do not take into account the presence of the ceramic particles, which explains the higher measured experimental velocity values. The experimental values are average velocities in the area of measurements (for PET, $V_L = 2540\ m\,s^{-1}$ and for silica, for instance, $V_L = 5970\ m\,s^{-1}$; $V_T = 3760\ m\,s^{-1}$; $V_R = 3410\ m\,s^{-1}$). The area scanned for $V(z)$ acquisition is always larger than the area of typical regions chosen to carry out the measurements. The acoustic signature of unbonded areas therefore can consist of one or two arches.

6. Conclusions

The high frequency acoustic microscopy technique is well suited to the characterization of the adhesive behaviour between PET films and a very thin layer of aluminium.

The acoustic images of the samples show a very rich contrast behaviour. The sensitivity of the technique has allowed us to gain insights into the surface phenomena produced by heat treatments greater than 200 °C. It offers a non-destructive means to control the size, density and distribution of ceramic particles and also the evolution of the crystallization with thermal processing conditions. The variation of the adhesion with the thermal treatment has been observed as a function of the number of unbonded areas. These zones have been characterized as losses of adhesion between the layer of aluminium and the PET film. No other type of adhesion defect, such as soft contact, slippery contact or imperfect contact, has been observed. The adhesion can thus be characterized by the area and the number of very localized unbonded areas.

References

1. F. AUGEREAU, B. CROS and J. P. MARCO, *Appl. Surf. Sci.* **99** (1996) 293.
2. E. DIEULESAINT and D. ROYER, "Ondes elastiques dans les solides" (Masson et Cie, Paris, 1974).
3. R. J. M. da FONSECA, Y. M. B. de ALMEIDA, B. CROS, J. M. SAUREL and M. J. M. ABADIE, *Thin Solid Films* **251** (1994) 110.
4. J. J. HUNSINGER, L. SIMONIN, J. P. GONNET, B. CROS and D. J. LOUGNOT, *Pure Appl. Optics* **4** (1995) 529.
5. R. J. M. da FONSECA, L. FERDJ-ALLAH, G. DESPAUX, A. BOUDOUR, L. ROBERT and J. ATTAL, *Adv. Mater.* **5** (1993) 508.
6. B. CROS, E. GAT and J. M. SAUREL, *J. Non-Cryst. Solids* (1997) (in press).
7. R. J. M. da FONSECA, J. M. SAUREL, A. FOUCARAN, E. MASSONE, T. TAGLIERCIO and J. CAMASSEL, *Thin Solid Films* **255** (1995) 155.
8. A. BRIGGS, "Acoustic microscopy" (Clarendon, Oxford, 1992), 103.
9. H. HAIDARA, M. F. VALLAT, P. MARTZ and J. SCHULTZ, *Eur. Polym. J.* **29** (1993) 899.
10. P. ZIEGLER, M. F. VALLAT, H. HAIDARA and J. SCHULTZ, *J. Mater. Sci.* (1997) (in press).
11. P. ZIEGLER, Thèse de Doctorat Mulhouse (1994).

Received 23 February
and accepted 19 December 1996